http://dx.doi.org/10.15576/GLL/2020.2.93

GLL

Geomatics, Landmanagement and Landscape No. 2 • 2020, 93–110

DATA CLASSIFICATION BASED ON PHOTOGRAMMETRY

Izabela Piech, Tadeusz Żaba, Aleksandra Jankowska

Summary

The aim of the paper was to classify data from aerial laser scanning and CIR digital images, which were orientated, connected and aligned by the Agisoft Photoscan software. Then, in order to distinguish the ground a point cloud was generated. This was to create a correct terrain mesh and, in consequence, an orthophotomap. The next stage is to develop a new point cloud using ArcGIS. The land cover from the images was combined with the ground mapped by LiDAR. New heights were calculated relative to the ground surface height 0. The point cloud was converted into a raster form, providing a normalized Digital Surface Model (nDSM). It was the first element of the output composition, which also consisted of the NIR and RED channels, acquired from the cloud point generated in Agisoft. The colour composition obtained in such way was subjected to four object-oriented and pixel-oriented classification methods: I – ISO Cluster, II – Maximum Likelihood, III – Random Trees, IV – Support Vector Machine. Object grouping is possible due to information stored in the display content. This technique is prompted by human ability of image interpretation. It draws attention to more variables, so effects similar to human perception of reality are possible to achieve. The unsupervised method is based on a process of automatic search for image fragments, which allows assigning them to individual categories by a statistical analysis algorithm. In turn, supervised method uses "training datasets", which are used to "teach" the program assigning individual or grouped pixels to classes [Benz UC et al., 2004]. The area studied for land development was the Lutowiska municipality, in the Podkarpackie Voivodeship, Bieszczady County. As a result of the classification, 11 classes of terrain features were distinguished: class 0 – road infrastructure, class 1 – roads, class 2 – buildings, class 3 – waters, class 4 – meadows, class 5 – arable lands, class 6 – pastures, class 7 – high vegetation, class 8 – medium vegetation, class 9 – low vegetation, class 10 – quarry. The area of research covers an area of about 28 km^2. Aerial images were made in 2015. Field vision and photopoint measurement was carried out in May 2018.

Keywords

laser scanning • aerial images • supervised classification • unsupervised classification

1. Introduction

In the era of modern technological progress and advancement of spatial data acquisition, we are observing an increase in use of digital photogrammetry and remote sens-

ing. The development in these fields of science has greatly facilitated and accelerated collecting and classifying data for conducting complex spatial analyses. This ubiquity of geoinformation has become so obvious that we do omit a simple question: where does it come from? Who, based on what data and how does generate this information? Photogrammetric methods are applied to create maps, and currently data are supplied to spatial information systems by creating topographic databases. This is accompanied by a development of aerial and satellite imaging – the main source of information about surrounding geospace [Kurczyński 2014]. Laser scanning is playing an increasingly important part, as it is slowly displacing the methods of measurement by traditional instruments. LIDAR is a much faster, feasible for large areas, more efficient and at the same time accurate method of development. Thanks to the integration of this data with footage obtained from aerial images, it is possible to gather information about land cover as well as its objects, and provide detailed analyses. These techniques are increasingly used, among others, to monitor changes in a natural and industrial environment, plant segmentation and methods of land use. They are also helpful, when preparing documentation for spatial planning, for distinguishing built-up areas and sites intended for development.

The combination of this type of data enables precise interpretation of an acquired image, and an automatic classification of field objects. An example of such use are both supervised and unsupervised methods of classification presented in this paper, performed in two ways: object-oriented and pixel-oriented analysis [Nagao 1980].

2. LiDAR technology

Data obtained from LiDAR present clear and valuable spatial information on objects, geometry and shape. They carry out an analysis and classification of an area with significant accuracy in a more efficient and automated way. LiDAR does not dependent on lighting conditions, the imaging is possible in the day and night (when digital camera recording is impossible). Laser scanning technique also allows direct data acquisition regardless of the weather (except fog and high cloud cover). This is due to its own light source. Despite short development time, it obtains data with very high altitude accuracy (0.10–0.15 m), while under certain conditions it can be reduced to 0.4–0.5 m.

An important advantage of this system is that it also does not depend on a type of surface. It easily penetrates through vegetation, which makes qualifying additional layers much easier.

Laser systems record the first, last or both reflections (echoes) [Pfeifer 2008]. In Polish conditions, aerial images can be taken over 50% of days a year. LiDAR technology has also a relatively low cost of obtaining data for large areas. The main disadvantage is an absorption of signals by clouds, fog, water and asphalt, and a large volume of datasets. Undoubtedly, this method and its equipment have great potential for further research.

3. Characteristics of the research area

The research area is a part of the Lutowiska municipality to the south-east of Podkarpackie Voivodeship. It is one of the three municipalities of the Bieszczady County and borders on the east with Ukraine and on the south with Slovakia. It belongs to the eastern flank of the European Union. Figure 1 presents its location against the background of the county, voivodeship and entire Poland.

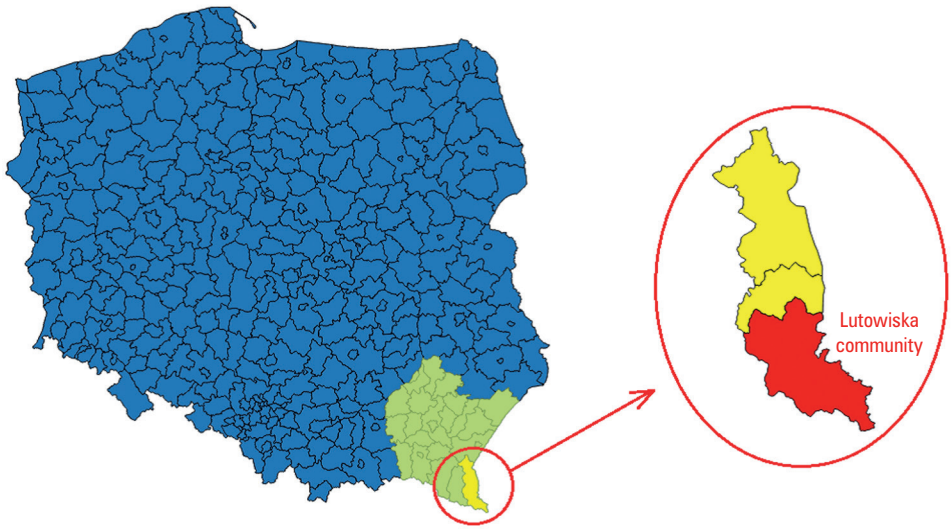

Source: Jankowska [2018]

Fig. 1. Location of the municipality against the background of the country, voivodeship and county

The area of study is entirely hilly, mostly covered with forests with high, medium and low vegetation. There are various terrain features such as: quarry, small water reservoirs, pastures, arable lands and low-rise buildings. Aerial imaging was done in 2015, field vision and photopoint measurement were performed in May 2018.

4. Input data

The input data are CIR aerial photographs taken in June 2015. They were used for further analysis of the facilities in the selected area of the Lutowiska municipality, which has grasslands, arable lands, forests of varying vegetation, built-up areas, quarry and water reservoirs. Due to the fact that it is a terrain with large height differences, aerial images were made at an approximate shooting height of 5000 m. As each photo was taken in a resolution of 13 080 × 20 010, assuming 25 cm pixels, an image covers about 16 km^2. The UltraCam Eagle camera was used for this purpose. Near-infrared radiation

registration provided photographs supplemented with multispectral information. An additional base are products from aerial laser scanning, which were used to generate DSM. These data were obtained from CODGiK2, however without photopoints, which were measured manually – the selection consisted in an unambiguous identification of details in the field and in the images. The equipment used was the Trimble GPS receiver, R8-3. High-quality footage allowed to generate an orthophotomap and to conduct a thorough analysis and classification of the area. The following programs were used in the development: Agisoft Photoscan, ArcGIS.

5. Procedure in Agisoft Photoscan

In the first stage, aerial footage, approximate camera coordinates, as well as aerial photos used for the development were imported (Fig. 2). The number of Key and Tie Points can be defined in the process of joining the images. Key Points are characteristic points found in each image. The user defines their maximum number. Interestingly, a larger amount does not guarantee higher accuracy of photo adjusting. On the contrary, it significantly extends the procedure and provides less amount of reliable elements that can be adopted in the alignment process. On the other hand, Tie Points take part in the alignment.

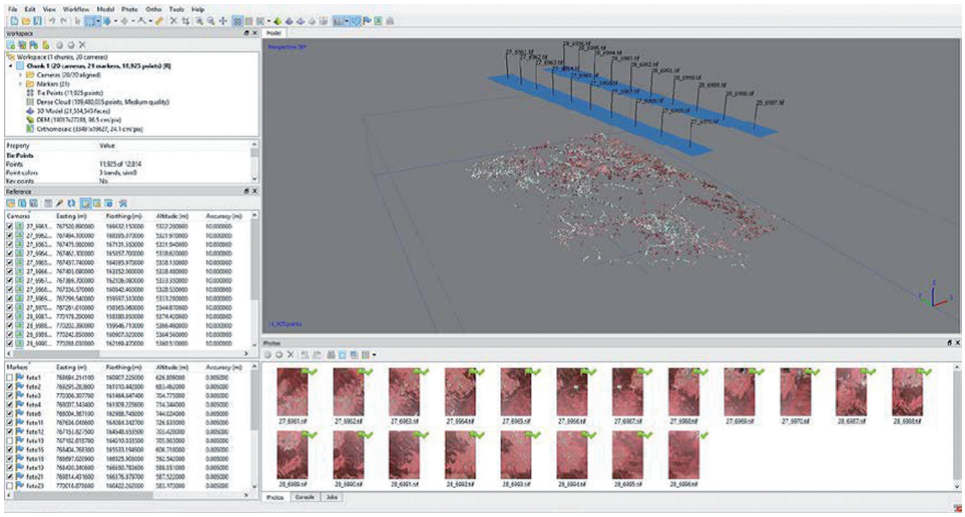

Source: Jankowska [2018]

Fig. 2. Importing images to the program

The final product of this stage is a sparse cloud point composed of Tie Points. The next step is to introduce field markers, which determine elements of external orientation by supplementing metricity and coordinate system (in case there are no coordinates of camera centres).

We can distinguish two situations in defining photopoints in images is a semi-automatic process:

1. The approximate system was defined by the coordinates of camera centres – after importing photopoint coordinates they appear in approximate locations on the images (accuracy about 5–10 m). The user corrects and confirms their location.
2. The coordinate system is not defined at all – photopoints have to be inserted manually. If the initial marker is indicated in the first photo, an adjacent line will automatically be generated on which it will be located. This method significantly facilitates unambiguous identification and correct insertion of a photopoint. If minimum two photopoints are indicated similarly on two photos and an optimization tool is used, then the photos will receive an approximate coordinate system, and the rest of the photopoints can be inserted as in point 1. For alignment, 20 photopoints were adopted, including 4 control points (Fig. 3). After performing camera optimization, which matched:
   - f – camera focal length,
   - cx, cy – coordinates of the main points of the photos,
   - k1, k2, k3 – radial distortion polynomial coefficients,
   - p1, p2 – tangential distortion polynomial coefficients,
   - an average error of alignment markers was 10.2 cm (4.3 cm on the X axis, 4.2 cm on the Y axis, 10.2 cm on the Z axis) and of control points was 12.5 cm (5.5 cm on the X, 4.4 on the Y axis, 12.5 cm to Z). Assuming a 25 cm pixel in each photo, the results obtained confirmed the exact procedure above.

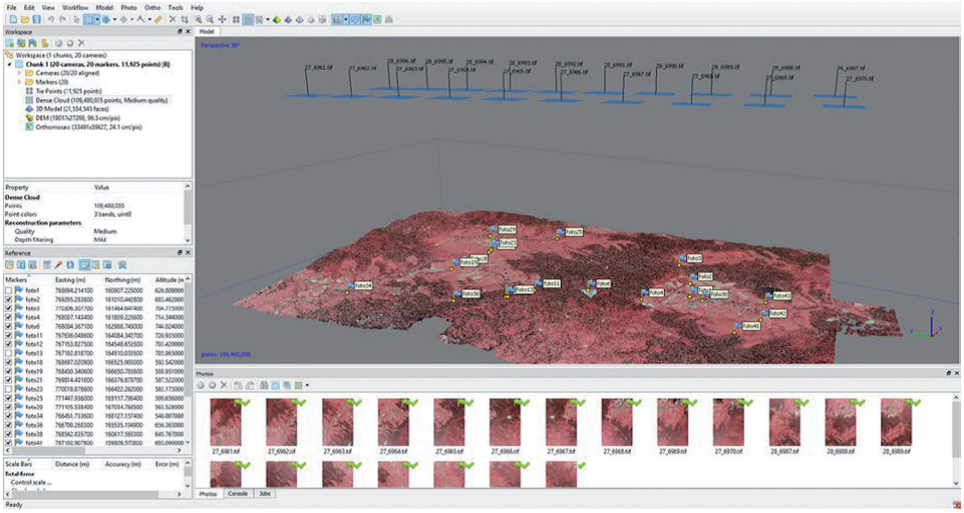

Source: Jankowska [2018]

Fig. 3. Photopoints adopted for alignment

The next step is to create a dense point cloud. During this process, side effect in form of measurement "noise" may occur. Depth filtering tool needs to selected in order to remove undesired by-product. The "aggressive" option is employed for aerial images, which is used for areas with no details. The generated point cloud (in 'medium' quality) consists of over 109 million points. To correctly generate a terrain mesh, it must be reclassified and discriminate the one that belongs to ground. Agisoft Photoscan allows to make such a classification (Fig. 4).

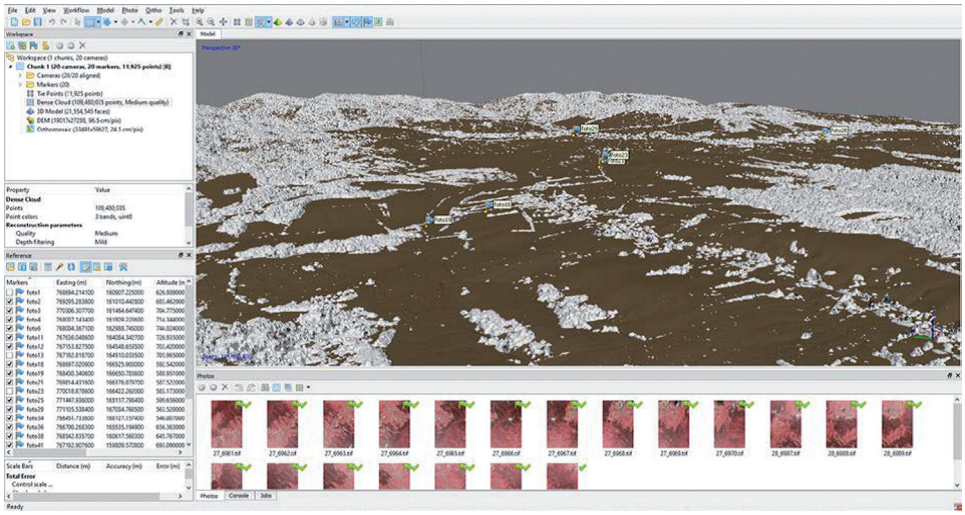

Source: Jankowska [2018]

Fig. 4. Ground surface classification

Then, after the cloud was classified, a mesh of triangles was created around the points of the terrain. Unlike LIDAR data, it does not designate terrain points to high bushes or trees. Therefore, the generated terrain in these spots may comprise large errors. In order to speed up the computer's work the program uses an algorithm to process aerial photos and generate heightfields (2.5D).

To avoid empty, unclassified spaces in the model, Photoscan allows to perform appropriate interpolation, due to which triangles with longer sides will be formed in spaces without assigned points. The final product is an orthophotomap from CIR images (Fig. 5).

As only ground points are classified, there may be slight displacements in all objects above the terrain line. To compensate for these errors, it is necessary to classify individual forms into appropriate classes, creating the so-called 'True ortho' and perform the orthorectification process.

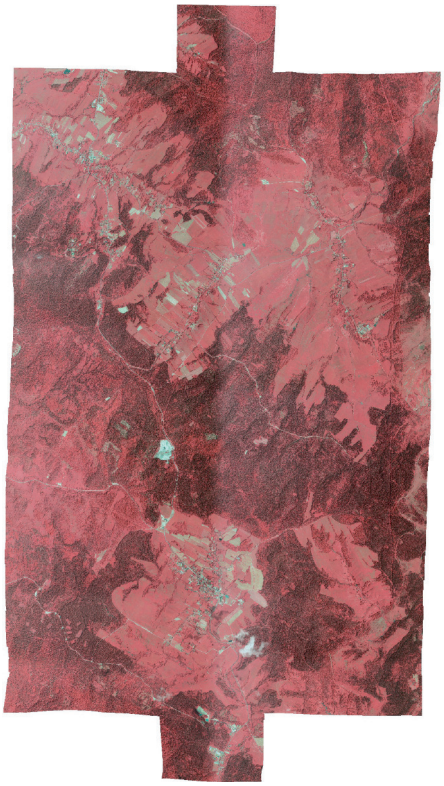

Source: Jankowska [2018]

Fig. 5. Orthophotomap from CIR photos

6. Procedure of preparing a composition for classification

The composition used in the classification consisted of three channels: nDSM (normalized Digital Surface Model), NIR channel and RED channel (Fig. 6).

The first channel was based on a point cloud obtained from stereographic images and another point cloud obtained from LiDAR. It was generated in PhotoScan and grouped into points that represented ground and those that represented land cover. Two point clouds were created, one with ground and one with land cover. The first was connected to the LIDAR cloud containing only ground. New heights were calculated for the newly created cloud (land cover from photos and terrain from LIDAR). Points representing the terrain received a height value equal to zero, and the height of rest of the elements was assigned relatively to it. Calculations related to the development of a standardized point cloud were run in the Lasmerge (Fig. 7a) and LasHeight (Fig. 7b) tools included in the LasTools program package. Then the point cloud was converted to a raster form, creating nDSM.

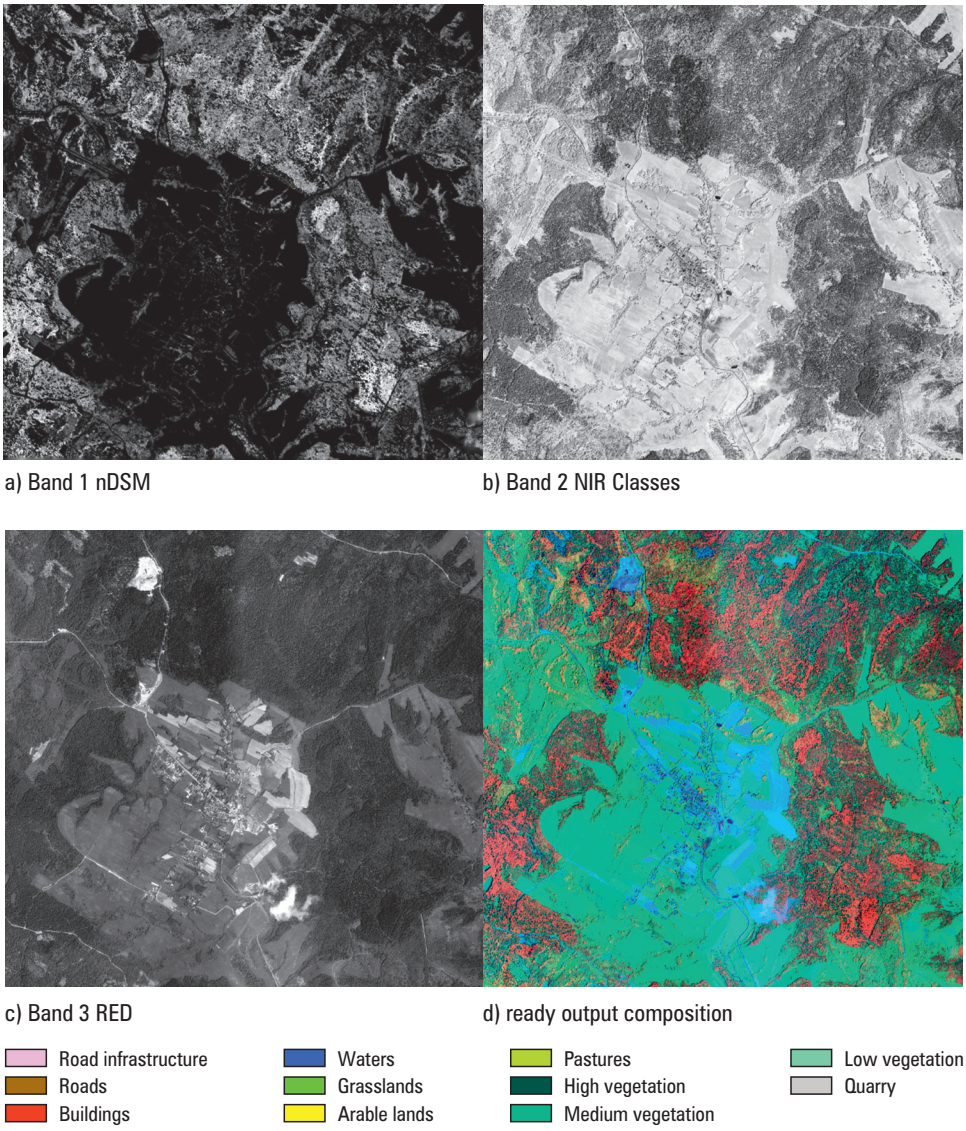

Source: Jankowska [2018]

Fig. 6. Elements of colour composition

To correct errors from the modification, the *Map Algebra tool* of ArcMAP program was applied. Negative values were replaced by zeros. Subsequently, the scale of height values was scaled to the range of 0–255 so that the values were identical to the values contained in the other two elements of composition. The second element of the composition was the NIR channel, which was obtained from an orthophotomap, created from

a point cloud in the AgiSoft program. The third element of the composition for classification, the RED channel, was also extracted from it. The *Make Raster Layer* (Fig. 7c) tool was used to distinguish individual channels. To create a composition consisting of three channels, *Composite Bands* was employed (Fig. 7d). All elements had the same pixel size of 0.25 cm. The finished composition (Fig. 8) was subjected to four classification methods: I – ISO Cluster, II – Maximum Likelihood, III – Random Trees, IV – Support Vector Machine.

Table 1 summarizes the results for the pixel-oriented method, and Table 2 – for the object-oriented method, which were exported from ArcGIS.

Approximately 15–20 polygons were created for each of 11 classes of terrain features were distinguished: class 0 – road infrastructure, class 1 – roads, class 2 – building, class 3 – waters, class 4 – meadows, class 5 – arable lands, class 6 – pastures, class 7 – high vegetation, class 8 – medium vegetation, class 9 – low vegetation, class 10 – quarry. Together, they constitute a study area of approximately 28 km^2.

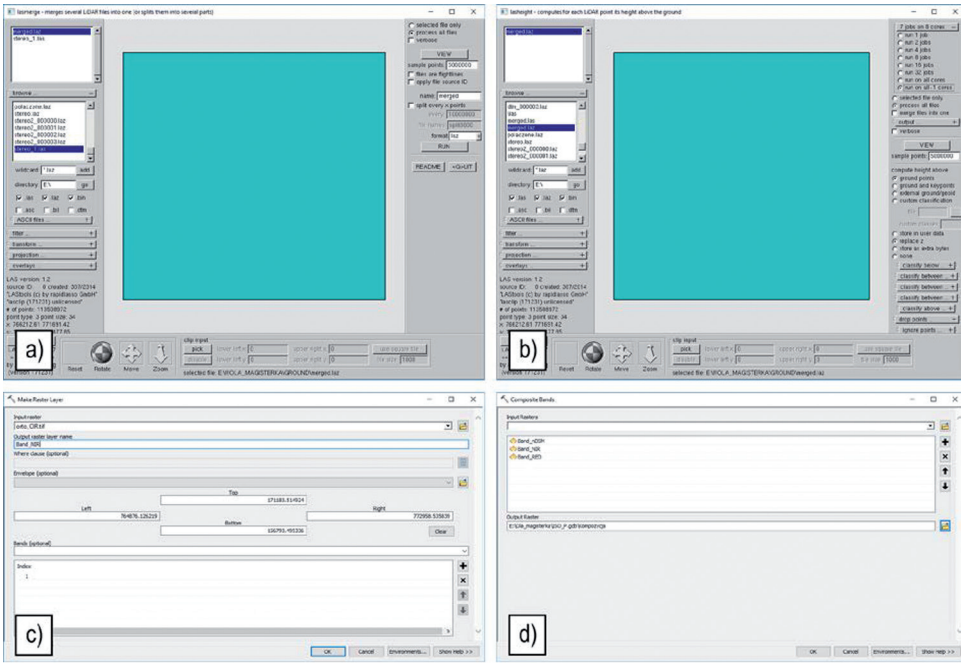

Source: Jankowska [2018]

Fig. 7. Tools used in ArcGIS

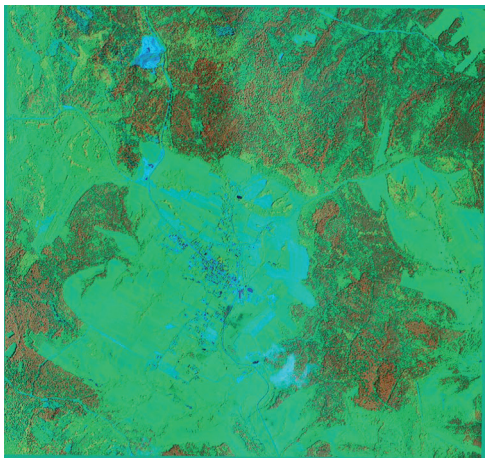

Source: Jankowska [2018]

Fig. 8. Output composition created from nDSM, NIR and RED

Table 1. Results for the pixel-oriented method

	Number of pixels (0.25 m pixel)			
	Method I	**Method II**	**Method III**	**Method IV**
road infrastructure	–	170788	334093	242872
roads	–	1685409	1606927	1619021
buildings	–	13609900	13052781	1993285
waters	–	1875992	3102660	1819191
grasslands	–	17556211	14456777	17897403
arable lands	–	2846139	10708199	1039977
pastures	166424648	133329938	123911761	115471093
high vegetation	257712885	92100156	94892376	86863491
medium vegetation	29298352	115089248	84686372	117033858
low vegetation	–	73961468	104999115	106619166
quarry	–	1210636	1684824	2836528
	Area [m²]			
	Method I	**Method II**	**Method III**	**Method IV**
road infrastructure	–	10674	20881	15180
roads	–	105338	100433	101189
buildings	–	850619	815799	124580

waters	–	117250	193916	113699
grasslands	–	1097263	903549	1118588
arable lands	–	177884	669262	64999
pastures	10401541	8333121	7744485	7216943
high vegetation	16107055	5756260	5930774	5428968
medium vegetation	1831147	7193078	5292898	7314616
low vegetation	–	4622592	6562445	6663698
quarry	–	75665	105302	177283
	Area [km²]			
	Method I	**Method II**	**Method III**	**Method IV**
road infrastructure	–	0.0107	0.0209	0.0152
roads	–	0.1053	0.1004	0.1012
buildings	–	0.8506	0.8158	0.1246
waters	–	0.1172	0.1939	0.1137
grasslands	–	1.0973	0.9035	1.1186
arable lands	–	0.1779	0.6693	0.0650
pastures	10.4015	8.3331	7.7445	7.2169
high vegetation	16.1071	5.7563	5.9308	5.4290
medium vegetation	1.8311	7.1931	5.2929	7.3146
low vegetation	–	4.6226	6.5624	6.6637
quarry	–	0.0757	0.1053	0.1773

Source: Jankowska [2018]

Table 2. Results for the object-oriented method

	Number of pixels (0.25 m pixel)			
	Method I	**Method II**	**Method III**	**Method IV**
road infrastructure	–	46100147	0	0
roads	–	1011344	69003	52262
buildings	–	6911128	8074215	1450835
waters	–	14218241	9626747	1516017
grasslands	29617867	15728344	20836868	21379057
arable lands	–	334255	22426	1469085

Table 2. cont.

pastures	146963651	134578852	143120305	145810459
high vegetation	131754052	97077063	74086609	91539738
medium vegetation	98094928	93398184	129109261	105403728
low vegetation	47005387	43363392	63538424	80375159
quarry	–	714935	4952027	4439545
	Area [m²]			
	Method I	**Method II**	**Method III**	**Method IV**
road infrastructure	–	2881259	0	0
roads	–	63209	4313	3266
buildings	–	431946	504638	90677
waters	–	888640	601672	94751
grasslands	1851117	983022	1302304	1336191
arable lands	–	20891	1402	91818
pastures	9185228	8411178	8945019	9113154
high vegetation	8234628	6067316	4630413	5721234
medium vegetation	6130933	5837387	8069329	6587733
low vegetation	2937837	2710212	3971152	5023447
quarry	–	44683	309502	277472
	Area [km²]			
	Method I	**Method II**	**Method III**	**Method IV**
road infrastructure	–	2.8813	0.0000	0.0000
roads	–	0.0632	0.0043	0.0033
buildings	–	0.4319	0.5046	0.0907
waters	–	0.8886	0.6017	0.0948
grasslands	1.8511	0.9830	1.3023	1.3362
arable lands	–	0.0209	0.0014	0.0918
pastures	9.1852	8.4112	8.9450	9.1132
high vegetation	8.2346	6.0673	4.6304	5.7212
medium vegetation	6.1309	5.8374	8.0693	6.5877
low vegetation	2.9378	2.7102	3.9712	5.0234
quarry	–	0.0447	0.3095	0.2775

Source: Jankowska [2018]

Method I – Unsupervised classification – ISO Luster
Method II – Supervised classification – Maximum Likelihood
Method III – Supervised classification – Random Teres
Method IV – Supervised classification – Support Vector Machine

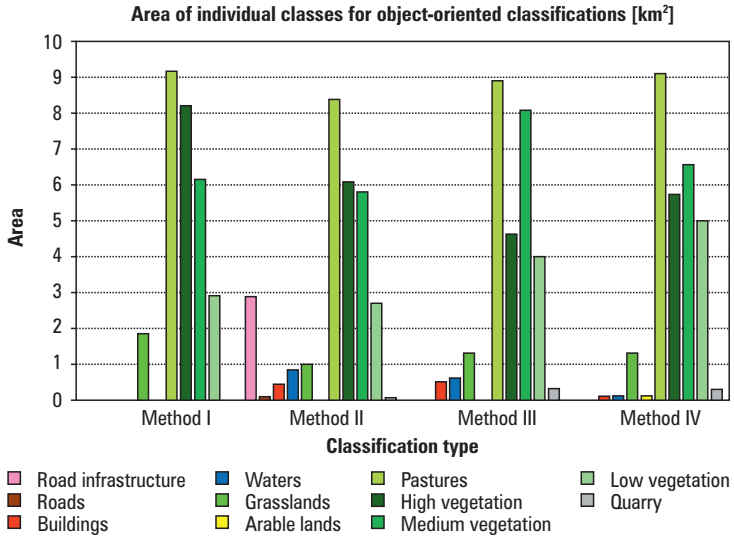

Source: Jankowska [2018]

Fig. 9. List of areas of individual classes for object-oriented classifications

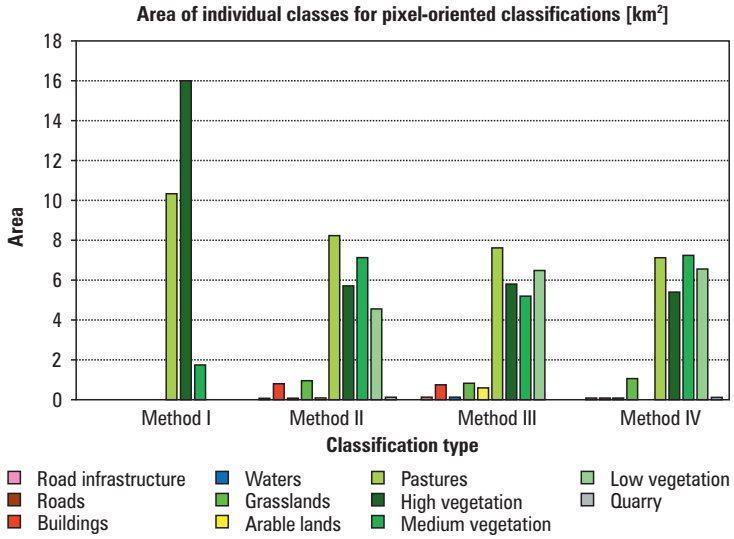

Source: Jankowska [2018]

Fig. 10. List of areas of individual classes for pixel-oriented classifications

From the Figures 9 and 10 and the lists of areas of individual classes (Tables 1 and 2) it follows that the unsupervised classification of ISO Cluster did not provide with intended results. As it only uses statistical analysis to assigns image elements to given categories, it does not identify clearly such elements as buildings, waters, arable lands, roads, road infrastructure or quarry. If the classification was obscure, it was necessary to decide individually to which class the object should be assigned based on the knowledge acquired in the field vision. In object-oriented methods, the whole scope of the study was divided between pastures (32%), high (29%), medium (22%) and low vegetation (10%), as well as meadows (7%). The difference is particularly visible in the fragment depicting the centre of the village (Fig. 11), where all the buildings were included in the meadows and medium-growing vegetation.

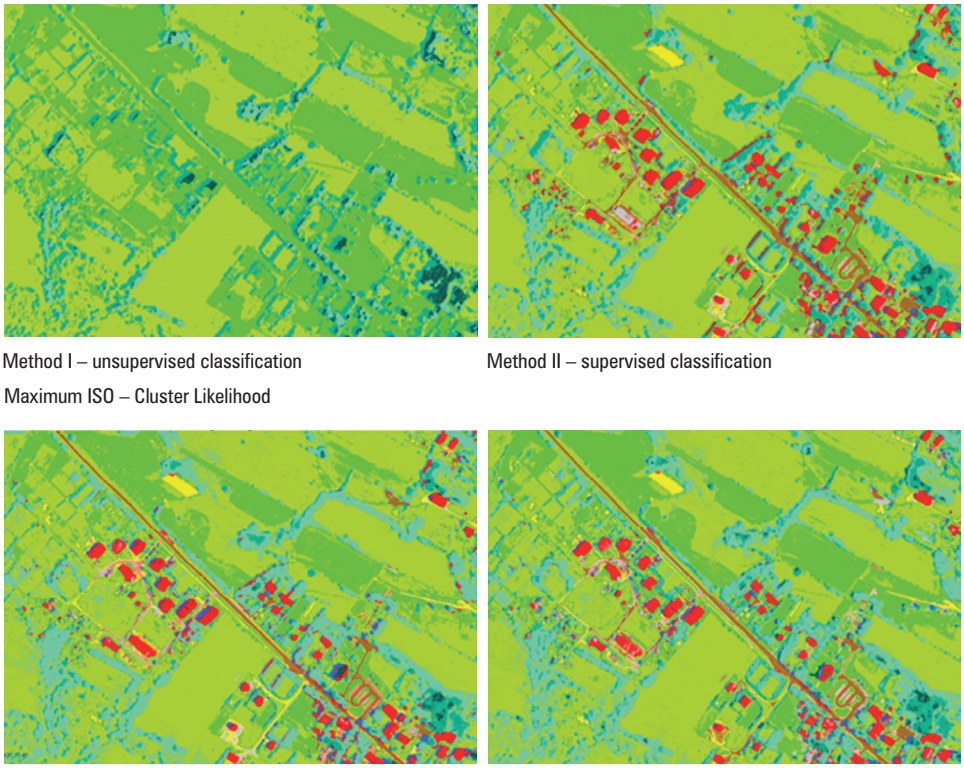

Method I – unsupervised classification
Maximum ISO – Cluster Likelihood

Method II – supervised classification

Method III – supervised classification
Random Trees Support Vector Machine

Method IV – unsupervised classification

Source: Jankowska [2018]

Fig. 11. Classification methods

The pixel grouping algorithm extracts even fewer classes compared to object-oriented algorithm. Among them, high vegetation, covering 16.11 km^2 (constituting 57%) dominates, followed by the pasture class with 10.40 km^2. Clearly visible medium vegetation covers an area of 1.83 km^2. Comparing both classifications, it can be noticed that the pixel-oriented method (Fig. 12) has high vegetation and pasture there where buildings stood in the actual place.

Subsequent methods present results more approximate to actual land use. In the Likelihood Maximum object-oriented method, pastures dominate occupying 30% of the total area with 8.41 km^2 (Fig. 13).

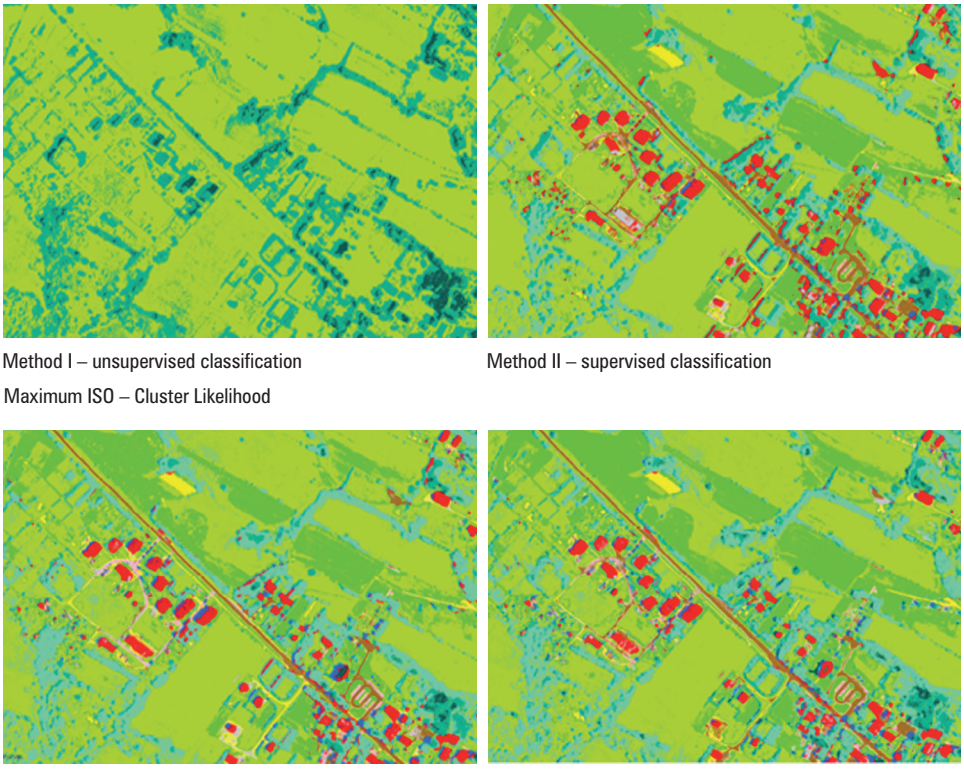

Method I – unsupervised classification

Maximum ISO – Cluster Likelihood

Method II – supervised classification

Method III – supervised classification

Random Trees Support Vector Machine

Method IV – unsupervised classification

Source: Jankowska [2018]

Fig. 12. Comparison of classifications

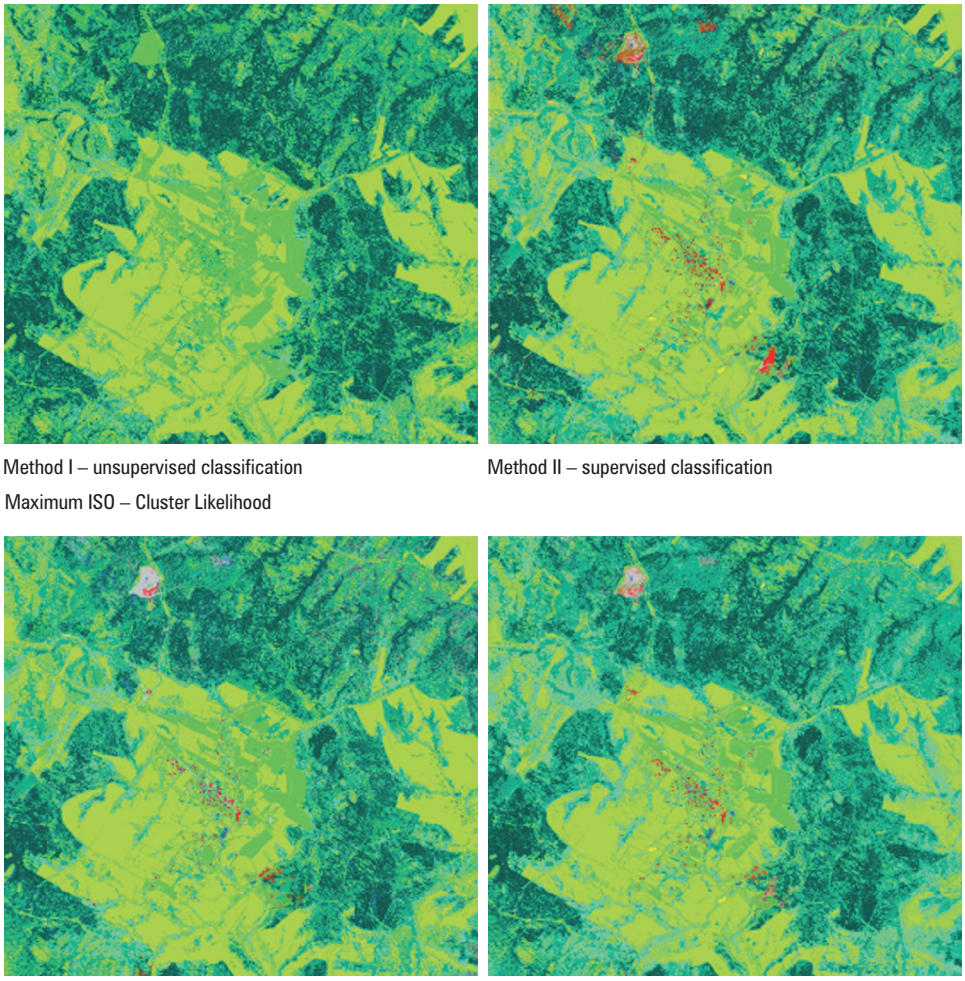

Method I – unsupervised classification
Maximum ISO – Cluster Likelihood

Method II – supervised classification

Method III – supervised classification
Random Trees Support Vector Machine

Method IV – unsupervised classification

Source: Jankowska [2018]

Fig. 13. Actual land use

The algorithm also captured large areas covered with high (6.07 km^2) and medium vegetation (5.84 km^2), which is found in the studied area. It manage to render very accurately road infrastructure (pavements, cobblestones, parking lots) as well as the road itself. However, spots shaded by trees posed some problems as the program classified them as water. This occurs because red light reflection is similar for asphalt and water table. Random Trees object-oriented technique accurately reproduces the varied tree stands, the ground between them, finding individual shrubs and correctly classify-

ing them. Similarly, only this program has correctly assigned almost the entire quarry located in the research area. However, it does not work with roads, which is clearly seen in Figure 14.

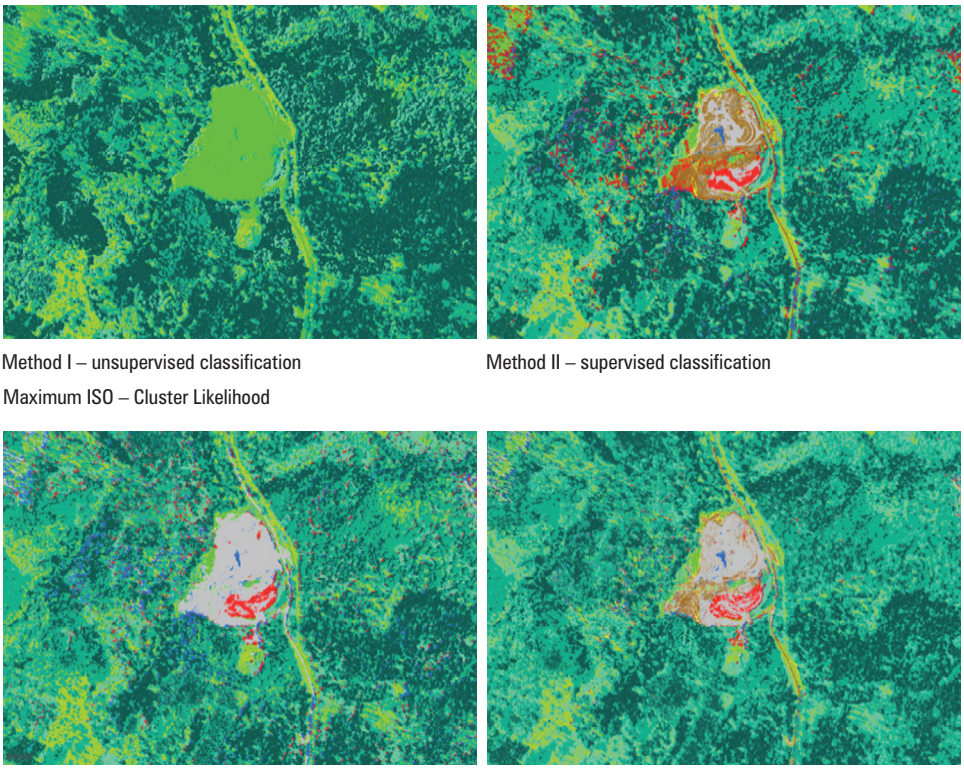

Method I – unsupervised classification
Maximum ISO – Cluster Likelihood

Method II – supervised classification

Method III – supervised classification
Random Trees Support Vector Machine

Method IV – unsupervised classification

Source: Jankowska [2018]

Fig. 14. Result of the road classification

A similar result was also obtained in the Support Vector Machine. There is a clear dominance of pastures (30–32%), medium and high vegetation (for Support Vector Machine medium vegetation 23% and high 20% respectively; Random Trees: 28% medium and 16% high). The IV pixel-oriented method also proved to be the best for correct classification of arable lands in places where they actually occur. Roads were the smallest area (in the area 0.0708 km^2, in the pixel 0.3070 km^2), road infrastructure (in the pixel 0.0467 km^2, in the area 2.8813 km^2) and arable lands (in the object-oriented 0.141 km^2, in the pixel-oriented 0.9121 km^2).

7. Conclusions

In result of the object-oriented and pixel-oriented classifications the following number of classes were obtained: for method I (unsupervised) with object-oriented approach: 5 classes (grasslands, pastures, high, medium and low vegetation); and with pixel-oriented approach: 3 classes (pastures, high and medium vegetation); for methods II, III and IV, both object- and pixel-oriented: 11 classes. The aim was to gather information on actual land use and land cover. The results of this analysis showed that ISO Cluster unsupervised classification was not effective in identifying and distinguishing individual terrain objects. The reason for its failure was that it used statistical analysis. It extracted elements with similar height, without distinguishing what class they belong to. Hence, buildings were assigned to high and medium vegetation, which obviously did not correspond to the reality. The accurateness of classification was verified by raster form to which the obtained image with class mapping of land use was compared. It cannot be asserted that object-oriented method was better only on the basis of a few cases, because in other cases the pixel-oriented method gave better results.

References

Benz U.C., Hofmann P., Willhauck G., Lingenfelder I., Heynen M. 2004. Multiresolution, object-oriented fuzzy analysis of remote sensing data for GIS-ready information. ISPRS Journal of Photogrammetry & Remote Sensing.

Everaerts J. 2008. The use of UAVs for remote sensing and mapping. ISPRS, Bejing.

Kurczyński Z. 2014. Fotogrametria. Wydawnictwo Naukowe PWN, Warszawa.

Nagao T. 1980. A structural analysis of complex aerial photographs. Tokio.

Pfeifer N. 2008. Strip Adjustment and DSM Computation, International School on Lidar Technology IIT Kanpur, India.

http://www.gugik.gov.pl/__data/assets/pdf_file/0020/23762/WYKLAD-9.pdf

http://progea.pl/satalitarny-skaning-laserowy-sls-satellite-laser-scanning/

Dr inż. Izabela Piech
Uniwersytet Rolniczy w Krakowie
Katedra Geodezji Rolnej, Katastru i Fotogrametrii
ul. Balicka 253a, 30-198 Kraków
e-mail:rmpiech@cyf-kr.edu.pl
ORCID: 0000-0002-6710-4387

Dr inż. Tadeusz Żaba
Politechnika Krakowska
Katedra Wodociągów, Kanalizacji i Monitoringu Środowiska
ul. Warszawska 24, 31-155 Kraków
e-mail: tadeusz.zaba@interia.pl
ORCID: 0000-0002-0967-164X

Aleksandra Jankowska
Graduate of the Faculty of Environmental Engineering and Land Surveying